Large eddy simulation of flow over a wooded building complex

R. G. Rehm[†], K. B. McGrattan[‡] and H. R. Baum[‡†]

*Building and Fire Research Laboratory, National Institute of Standards and Technology,
Gaithersburg, MD 20899, U.S.A.*

Abstract. An efficient large eddy simulation algorithm is used to compute surface pressure distributions on an eleven story (target) building on the NIST campus. Local meteorology, neighboring buildings, topography and large vegetation (trees) all play an important part in determining the flows and therefore the pressures experienced by the target. The wind profile imposed at the upstream surface of the computational domain follows a power law with an exponent representing a suburban terrain. This profile accounts for the flow retardation due to friction from the surface of the earth, but does not include fluctuations that would naturally occur in this flow. The effect of neighboring buildings on the time dependent surface pressures experienced by the target is examined. Comparison of the pressure fluctuations on the single target building alone with those on the target building in situ show that, owing to vortices shed by the upstream buildings, fluctuations are larger when such buildings are present. Even when buildings are lateral to or behind the target, the pressure disturbances generate significantly different flows around this building. A simple grid-free mathematical model of a tree is presented in which the trunk and the branches are each represented by a collection of spherical particles strung together like beads on a string. The drag from the tree, determined as the sum of the drags of the component particles, produces an oscillatory, spreading wake of slower fluid, suggesting that the behavior of trees as wind breakers can be modeled usefully.

Key words: computational fluid dynamics; computational wind engineering; large eddy simulations; tree(single) drag model.

1. Introduction

Due to the revolutionary increase in computer power and the evolutionary improvement in algorithms for computational fluid dynamics, computational wind engineering (CWE) has become a useful tool for the exploration of wind effects on structures. While full-scale and wind-tunnel measurements have traditionally been the primary guides for the wind engineer, these measurements can now be usefully supplemented by CWE. One of the advantages of computations is that the engineer can economically assess the effect of nearby structures and trees, for example, on the pressure distribution experienced by a "target" building.

This study shows that the pressures experienced by a building are strongly dependent upon the specific site on which this building is located. Local meteorology, neighboring buildings, topography and large vegetation (trees) all play an important part in determining the flows and therefore the

† Ph.D., NIST Fellow
‡ Ph.D., Research Mathematician
‡† Ph.D., NIST Fellow

pressures experienced by the target. We have chosen the campus of our institution, NIST, as the site to study since it is composed of a cluster of ten buildings surrounded at some distance by an equal number of additional buildings and an expanse of relatively open fields. Beyond its 233 hectare campus is a modern suburban region with many homes and some medium-rise buildings. The topography is gently rolling hills, and some of the trees are taller than any building on campus except the target building. We have only investigated the local meteorology to the extent that we consider a typical mean atmospheric boundary layer generated by winds coming generally from the west or from the northwest. Currently, there are no on-campus measurements of wind pressures or velocities which would be useful for comparison with computational results, but plans for such measurements are underway.

In this paper, we first present briefly the mathematical model (the Navier-Stokes equations with body forces) and the algorithm used for its solution. Next, results are shown for two base computations, one with only the target building (the 11-story Administration building) and the other with the target building plus several adjacent buildings. The qualitative difference is illustrated by pictures of average streamlines over these two configurations, with quantitative differences showing up in pressure and velocity probe measurements at various locations on this portion of the campus. Then a simple mathematical model for the drag produced by an individual tree is introduced and consequences of this grid-free model are investigated. Finally, a summary and conclusions are given.

2. Model and LES methodology

The flow is governed by the incompressible Navier-Stokes equations :

$$\nabla \cdot \boldsymbol{u} \, = \, 0 \tag{1}$$

$$\frac{\partial \boldsymbol{u}}{\partial t} + \nabla(v^2/2) - \vec{v} \times \vec{\omega} + \nabla p \, = \, \boldsymbol{f} + \frac{1}{Re}\,\nabla^2 \vec{v} \tag{2}$$

The first of these equations is a statement of the conservation of mass, which for an incompressible fluid is equivalent to conservation of volume. The second, vector equation is the statement of conservation of momentum. Here, all symbols have their usual fluid dynamical meaning : $\vec{v} = \boldsymbol{u}$ is velocity, p is pressure and $\vec{\omega} = \nabla \times \vec{v}$ is the vorticity. In addition, t is time, ∇ is the spatial gradient, divergence or curl operator and $\boldsymbol{f}$ is the body force per unit mass. All quantities have been made dimensionless, the lengths relative to a length scale H determined by the height of the target building, the velocity relative to a scale V_0 determined by the incoming flow, the pressure relative to the dynamic pressure $(\rho V_0^2 / 2)$ and the time relative to the length scale and the velocity scale. Here, Re is the Reynolds number, $V_0 H / v$, where v is the kinematic viscosity.

To obtain the pressure, we take the divergence of the momentum equation rewritten as follows :

$$\frac{\partial \boldsymbol{u}}{\partial t} + \boldsymbol{F} + \nabla \mathcal{H} \, = \, 0 \tag{3}$$

where $\mathcal{H}$ is defined to be the total pressure divided by ρ_∞ :

$$\mathcal{H} \, = \, \frac{v^2}{2} + \frac{\tilde{p}}{\rho_\infty} \tag{4}$$

and where

$$\boldsymbol{F} = -\left(\vec{v} \times \vec{\omega} + \boldsymbol{f} + \frac{1}{Re}\nabla^2\vec{v}\right)$$

All the convective and diffusive terms have been incorporated in the term $\boldsymbol{F}$. The resulting equation for $\mathcal{H}$ is an elliptic partial differential equation

$$\nabla^2\mathcal{H} = -\nabla \cdot \boldsymbol{F} \tag{5}$$

The linear algebraic system arising from the discretization of Eq. (5) has constant coefficients and can be solved to machine accuracy by a fast, direct (i.e., non-iterative) method that utilizes fast Fourier transforms (Swarztrauber and Sweet 1975). No-flux boundary conditions (BCs) are specified by asserting that along the normal n

$$\frac{\partial\mathcal{H}}{\partial n} = -F_n \tag{6}$$

at solid walls, where F_n is the normal component of $\boldsymbol{F}$ at the wall. This equation asserts that the normal component of velocity at the wall does not change with time, and indeed remains zero assuming the flow velocity is initially zero. At open external boundaries it is assumed that the perturbation pressure is zero, but there are other strategies for prescribing open boundary conditions that will not be discussed here.

Direct Poisson solvers are most efficient if the domain is a rectangular region, and the no-flux condition (6) is simple to prescribe at external boundaries. However, internal obstructions may be included in the overall domain as masked grid cells, but the no-flux condition (6) cannot be directly prescribed at the boundaries of these blocked cells due to consistency issues. However, it is possible to exploit the relatively small changes in the pressure from one time step to the next to enforce the no-flux condition. At the start of a time step, the components of the convection/diffusion term $\boldsymbol{F}$ are computed at all cell faces that do not correspond to walls. Then, at those cell faces that do, set

$$F_n = -\frac{\partial\mathcal{H}^*}{\partial n} + \beta u_n \tag{7}$$

where F_n is the normal component of $\boldsymbol{F}$ at the wall, and β is a relaxation factor empirically determined to be about 0.8 divided by the time step. The asterisk indicates the most recent value of the pressure. Obviously, the pressure at this particular time step is not known until the Poisson equation is solved. Eq. (7) asserts that following the solution of the Poisson equation for the pressure, the normal component of velocity u_n will be driven closer to zero according to

$$\frac{\partial u_n}{\partial t} \approx -\beta u_n \tag{8}$$

This is approximate because the true value of the velocity time derivative depends on the solution of the pressure equation, but since the most recent estimate of pressure is used, the approximation is very good. Also, even though there are small errors in normal velocity at solid surfaces, the divergence of each blocked cell remains exactly zero for the duration of the calculation, and the consistency condition (5) ensures global mass conservation. In other words, the total flux into a given obstacle is always identically zero, and the error in normal velocity is usually at least 3 or 4 orders of magnitude smaller than the characteristic flow velocity. When implemented as part of a

predictor-corrector updating scheme, the no-flux condition at solid surfaces is maintained remarkably well. More details of both the formulation of the model and of the computational scheme can be found in McGrattan *et al.* (1998, 2000).

For uniform density flows, results can be expressed in terms of a pressure coefficient $C_p = (p - p_0) / (\rho_0 V_0^2 / 2)$. where p_0 is the ambient pressure, ρ_0 is the ambient air density, and V_0 is a velocity characterizing the prevailing steady wind. Positive pressure coefficients indicate pressures above ambient and negative ones below ambient. For uniform flow, V_0 is this velocity, while for a shear flow V_0 is taken to be the velocity at the building height. The velocity profile is taken to have the form

$$V(z) / V_0 = (z / H)^{1/n} \tag{9}$$

where H is a reference height, here taken to be the height of the building, V_0 is the reference velocity at that height and n is a number which varies with the roughness of the surface upstream of the building; the greater the roughness the smaller the value of n. The value 4 was selected here, and the reference velocity V_0 was taken to be 5 m/s.

We report an initial computational examination of the effects of neighboring buildings and trees on the flow fields experienced by a target building. We first note that buildings upstream of a target building have an important effect on the flow around the target building, since, generally, large vortical structures are shed intermittantly by the upstream buildings. Visualization of these dynamical effects are dramatic. However, even when the buildings are lateral or behind the target relative to the incoming wind, the pressure disturbances produced by these neighbors generate significantly different flows around this building. Therefore, it is essential to consider the actual site, as well as the wind conditions, when examining flows experienced by a target building. We compare two computations, one with the target building alone and the other with the target building together with its neighboring buildings (in situ). Then, we consider some effects of trees; the momentum reduction caused by an individual tree is examined first. Next, disturbances caused by a row of trees upstream of the target building alone is examined.

3. Target building alone and with neighboring buildings

Fig. 1 shows the average streamlines for flow over the NIST campus about 3 meters above the ground, first for the the administration building alone, the target building in this case, on the left and in its cluster of buildings on the right. Note the difference in complexity of the flow patterns between these two cases.

For the computations presented here, we have chosen either a constant effective kinematic viscosity ν which is just large enough to dissipate velocity variations at the resolution limits of the calculation, or the subgrid Smagorinsky turbulence model. In both cases, the grids used for the computations are able to resolve convective motion over a spatial range of nearly two orders of magnitude for the three-dimensional calculations. The computations are interpreted as Large Eddy Simulations (LES) with a constant subgrid eddy viscosity in the first case and with the Smagorinsky subgrid eddy viscosity in the latter. The total number of grid cells for these computations were in excess of 600,000 and have been carried out in each case on an engineering workstation over a period of between 15 and 24 CPU hours, depending upon the grid size and the number of minutes simulated.

The elliptic solver used for the computations permits the computational grid to be stretched in one
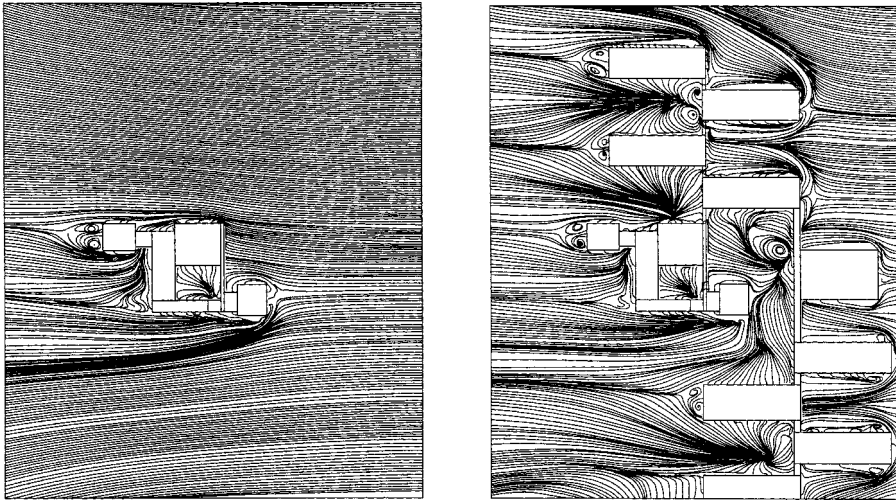
Fig. 1 Average streamlines for flow over the NIST campus. Administration building without and with surrounding buildings. North is down, and prevailing wind is from the west

or two coordinate directions (Swarztrauber and Sweet 1975). As noted above, the numerical scheme is very computationally efficient and accurate, requiring between 10 and 30 μs / grid-cell/time-step, depending upon the CPU used for the simulation. Computations of this resolution (millions of grid cells) usually require many days on a supercomputer, but these computations have been carried out in a fraction of that time on modern workstations and PCs. The efficiency and accuracy arise from a combination of factors, a very simple rectangular grid, internal objects that are described only by rectangular blockages and the direct pressure solver used. Details of the computational scheme can be found in McGrattan *et al.* (1998), (2000). Also, the code, known as the Fire Dynamics Simulator (FDS), can be downloaded free from the URL: http://fire.nist.gov. It consists of two components, a computational fluid dynamics (CFD) code, called fds, written in Fortran 90 for computation of fire-driven flows, and an OpenGL graphics program for visualization of results. Both codes run on PCs and several popular UNIX workstations.

Steady-state pressure coefficients on a single building determined from computations using a few million grid cells were reported in Rehm *et al.* (1999) and were found to compare very favorably with several experimental studies. In addition, the fds code has been used by Lim (2000) to evaluate the methodology for urban flow simulations by comparison with wind tunnel measurements of flows over rows of cubic obstacles representing a simple urban environment. His studies also indicate that the methodology and code are promising for such simulations.

In the simulations reported here, the computational domain is on the order of a kilometer per side: more generally let L be the length scale characterizing the computational domain. If the grid consists of a characteristic number of cells N in each direction (so that the total number of grid cells is O(N^3)), there are two length scales that characterize the simulations, the large scale domain size L and a small scale $l = O(L / N)$ that characterizes the grid size. The computation can at best resolve length scales x such that $l \leq x \leq L$. All lengths larger than L can not be treated, while all length scales of order l or smaller will not be resolved. Described in another way, the computations can be expected to resolve wavenumbers k between $1/L \leq k \leq 1 / l$ at best. Likewise, the computations can
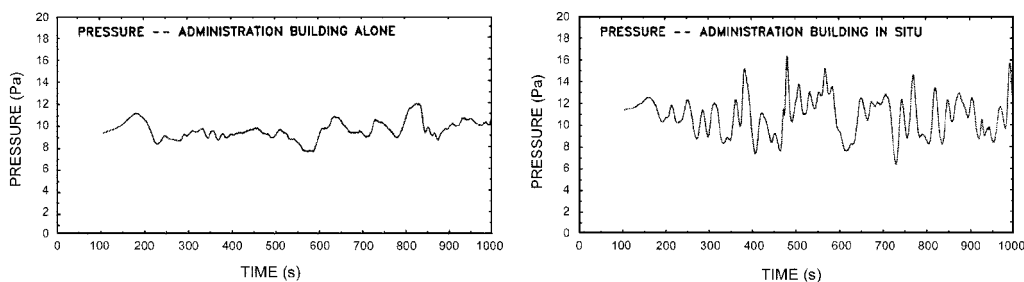
Fig. 2 Pressure versus time on the administration building without and with surrounding buildings
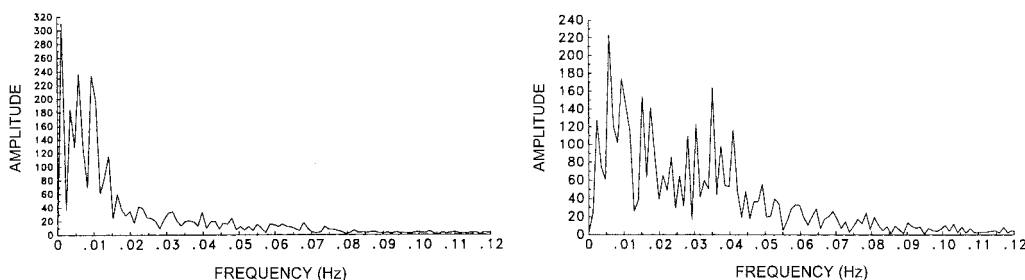

Fig. 3 Frequency spectrum from pressure probes on the center of the windward face of the administration building without and with surrounding buildings

be expected to resolve temporal fluctuations for time scales t in the range $l / V_0 \leq t \leq L / V_0$ at best. If local meteorology can provide pressure and velocity data on the boundary of the computational domain for length scales x between $l \leq x \leq L$ and for time scales t between $l / V_0 \leq t \leq L / V_0$, then the computations will at best be able to maintain this resolution during the simulation. Turbulence with length scales below l cannot be resolved whereas fluctuations with length scales somewhat greater than l will be resolvable and therefore are accounted for in the computations.

The effects of neighboring buildings on the pressures experienced by the target building are illustrated in Figs. 2 and 3. Fig. 2 shows pressure plots as functions of time determined from a probe at the center of the west (or windward) face of the target building. The plot on the left of Fig. 2 is the profile determined when the neighboring buildings are absent, while the plot at the right shows the corresponding profile when these buildings are present. Note that the right plot shows substantially larger pressure fluctuations. In Fig. 3 the Fourier transforms of the plots of Fig. 2 are shown. Note again that the frequency spectrum found when the neighboring buildings are present exhibits a broader band of lower frequencies. Vortices shed from the neighboring buildings drift over the target building inducing these larger, relatively low-frequency pressure variations.

4. Trees

Plants and trees exchange mass, momentum and energy with the atmosphere. Of interest in meteorology are the effects of forests on the local microclimate and, in turn, the effects of the local meteorological conditions on forests. The simplest modeling approach for these exchanges has been to assume the trees form a horizontally homogeneous canopy, so that atmosphere-forest interactions

can be modeled by one-dimensional transport in the vertical direction (Raupach and Thom 1981), (Gross 1993). Both the turbulence in the atmospheric boundary layer and the properties of the tree canopy determine this vertical transport. This 1-D model has yielded analytical solutions and computational results which have provided guidance and understanding of the interaction between forests and the atmosphere.

More detailed numerical modeling of the interaction of the trees with the atmosphere has utilized a recast form of the conservation equations using a Reynolds-Averaged-Navier-Stokes (RANS) approach (Gross 1993). In this approach, the equations of motion are averaged first, and then averages of higher order turbulent fluctuations must be related back to lower order averages through "closure" models or subgrid-scale turbulence models. Such modeling can be justified for steady, large-scale interactions between forests and the atmosphere, but is more difficult to justify for time dependent flows.

There has been much less effort devoted to the the study of the interaction of the atmosphere with individual trees (Johnson *et al*. 1981, Baker and Bell 1992, Roodbaraky *et al*. 1994, Gross 1993). Baker and Bell (1992), use a term which captures this distinction: they refers to "urban trees", or simply individual trees. A summary of numerical modeling as well as experiments on individual trees has been presented by Gross (1993). The numerical studies of individual trees have also used a RANS approach, assuming that the interaction is steady and computing these interactions down to a resolution of about a meter in the horizontal directions (Gross 1993).

Other experimental studies, not reported in Gross (1993), provide data on drag variation with wind speed. Johnson *et al.* (1981) measured the drag forces on each of two trees of three species of live dwarf conifers, white pines, cryptomeria and Alberta spruce. All of the trees were found to accommodate (bend and twist) as the wind increased, with the amount of accommodation being species dependent. In addition, Baker and Bell (1992) reports that, although earlier experiments of tree drag as a function of wind speed suggest that drag varies linearly, his experiments find a slight preference for a quadratic variation with wind speed.

More generally, in simulations of the built environment, both buildings and trees are discrete and must be treated individually. Length scales of the order of a meter must be resolved and the atmosphere-tree interaction must be treated as a time dependent process. Then, Large Eddy Simulations (LES), in which the equations of motion are averaged only over subgrid length scales, are preferable to a RANS formulation.

Based on these studies, we adopt a simple tree submodel valid for low wind speeds only in which the trees do not bend or twist. A momentum deficit, which may vary with time, is introduced by each tree into our Large Eddy Simulations as described below. It is expected that tree accommodation can be accounted for later using a more sophisticated submodel.

5. A grid-free model for tree drag

Since trees can be various sizes, and will generally occupy a (major perhaps) fraction of only a few cells, they must be modeled in a way that is independent of the particular grid employed. Furthermore, since Large Eddy Simulations are inherently time dependent, a quasi-steady formulation such as the RANS approach described above is not satisfactory. Rather, the trees introduce a momentum deficit or drag, which will be time dependent and must ultimately be calibrated with measurements at full or wind-tunnel scale. As a model for a tree, we propose a collection of point particles strung together as beads to form either the tree trunk or its branches. Fig. 4 shows a simple schematic diagram of how one of these trees might look. While these particles take the shape of the
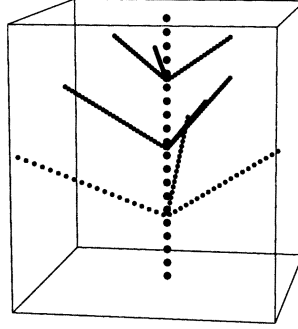
Fig. 4 schematic diagram of a grid-free tree composed of spherical particles strung together as beads to form
      the tree trunk and branches

tree trunk and branches, their drag must include that of the tree leaves or needles also.

   The body force term for the tree in the momentum equations is then determined by the
momentum transferred from the collection of particles to the gas. It is obtained by summing the
force transferred from each particle in a grid cell and dividing by the cell volume

$$f = \frac{1}{2} \frac{\sum C_d \pi r_d^2 (-u)|u|}{\delta x \delta y \delta z} \tag{10}$$

where C_d is a drag coefficient, u is the velocity of the gas, and $\delta x \delta y \delta z$ is the volume of the grid cell.
The drag coefficient is a function of the local Reynolds number Re_d. As a first step, the particles are
taken to be spheres, although alternative (more realistic) choices could be made. Thus,

$$C_D = \begin{cases} 24/Re_d & Re_d < 1 \\ 24(1 + 0.15\mathrm{Re}_d^{0.687})/Re_d & 1 < Re_d < 1000 \\ 0.44 & 1000 < Re_d \end{cases} \tag{11}$$

$$Re_d = \frac{\rho|u|2r_d}{\mu} \tag{12}$$

   Here, r_d is the radius of the individual sphere and μ is the dynamic viscosity of air. For a tree, the
size and the number of the spheres for each branch is specified, as well as the number of branches.
Similarly, the sphere size and number is specified for the tree trunk. This model assumes that the
aerodynamic drag of each component of the tree will vary quadratically with wind speed. We note,
however, that the wind profile in these simulations varies with height, and, therefore, the drag force
on each element will also vary with height, contrasting with the experimental results reported by
Johnson et al, for example, where the wind-tunnel flow is uniform with height.

6. Some effects of tree drag

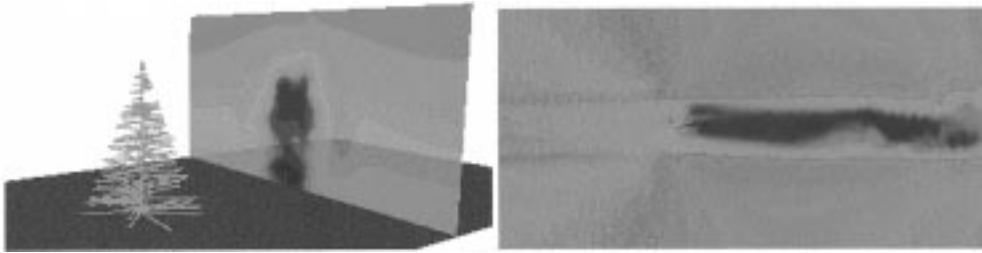   First, consider the wind flow over a large, single tree using the model described above. Fig. 5

Fig. 5 The velocity in the flow direction over a single large tree viewed in two ways. The left picture shows this velocity component in a plane normal to the flow direction and downstream of the tree. The right picture shows this velocity component from above in a horizontal plane at about one third the height of the tree. Red represents largest wind flows and blue lowest
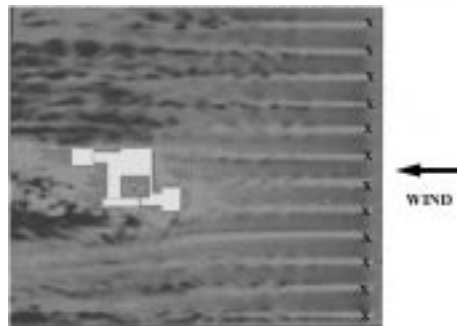

Fig. 6. The velocity in the flow direction over the target building with a row of model trees upwind. Here, blue represents the undisturbed flow at this level, green a reduced velocity component and red the lowest (or reversed flow) velocity compnent

shows the wake induced by the tree, in which the fluid is retarded relative to the ambient flow and oscillatory behavior develops. The retardation of the fluid confirms the well-known characteristic of trees to be "wind breakers". Since the model is grid free, much of the energy extracted by the branches, twigs, and leaves or needles from the flow is at the grid scale and, therefore, is rapidly dissipated.

Next, consider the effect of a row of trees upwind of the target building. (The building is 49 meters high, and the trees are taken to be 20 meters high.) Fig. 6 shows from above the velocity component in the direction of the wind at a height of 3 meters above the ground. This velocity component is denoted by the color blue at this height. Note the wakes of the trees, where the windward velocity component is reduced (shown in green). These wakes oscillate and spread laterally and produce fluctuations at low levels on the target building. However, they have relatively little effect on the pressure traces determined at the center and above on the windward face of the target building.

7. Conclusions

An algorithm was described for large eddy simulations of the inherently time-dependent flow around buildings. Computational domain and grid sizes determine the length scales of the flow features which can be resolved. The pressures experienced by a target building are strongly dependent upon the specific site on which the building is located. Local meteorology, neighboring

buildings, topography and large vegetation (trees) all play an important part in determining the flows and therefore the pressures experienced by the target. As expected, neighboring buildings were found to exert a very strong influence on the flow (and pressures) around the target; fluctuations were found to be larger when the neighboring buildings are present. Buildings upstream of the target were found to shed intermittently large vortical structures which pass over the target. However, even lateral or downwind buildings were found to produce pressure disturbances which generate significantly different flows around the target.

Finally, a simple grid-free mathematical model of a tree was presented; this model introduces drag which reduces momentum in the flow direction. Computations of the flow field over a single tree exhibited an oscillatory, spreading wake behind the tree. A row of trees upwind of the target building were found to change flow patterns at lower levels, but to have little effect on the pressures experienced on the upper levels of the target building.

Acknowledgements

References

Baker, C.J. and H.J. Bell (1992), "The aerodynamics of urban trees", *J. Wind Eng. Ind. Aerod.*, **41-44**, 2655-2666.

Johnson, R.C., Ramey, G.E. and O'Hagan, D.S. (1981), "Wind induced forces on trees", Paper 81-WA/FE-7, Fluids Engineering Division of the American Society of Mechanical Engineers, Winter Annual Meeting, November 15-20, 1981, Washington, D.C.

Lim, David, Private communication: Titan Corporation, Titan Research and Technology Division Internal Reports, "Validation of the NIST LES for Urban Flow Simulations", September 28, 1999 and "Evaluation of the LES Code for Urban Flow Simulations. Part II", March 3, 2000.

McGrattan, K.B., H.R. Baum and R.G. Rehm, (1998), "Large eddy simulations of smoke movement", *Fire Safety J.*, **30**, 161-178.

McGrattan, K.B., H.R. Baum, R.G. Rehm, A. Hamins and G.P. Forney, "Fire dynamics simulator - technical reference manual", NISTIR 6467, National Institute of Standards and Technology, January 2000.

Raupach, M.R. and A.S. Thom (1981), "Turbulence in and above plant canopies", *Annual Reviews of Fluid Mech.*, **13**, 97-129.

Gross, Gunter, *Numerical Simulations of Canopy Flows*, Springer-Verlag, New York, 1993.

Rehm, R.G., K.B. McGrattan, H.R. Baum and E. Simiu, "An efficient large eddy simulation algorithm for computational wind engineering: Application to surface pressure computations on a single building", NISTIR 6371, National Institute of Standards and Technology, August 1999.

Roodbaraky, H.J., C.J. Baker, A.R. Dawson and C.J. Wright (1994), "Experimental observations of the aerodynamic characteristics of urban trees", *J. Wind Eng. Ind. Aerod.*, **52**, 171-184.

Simiu, Emil and Robert H. Scanlan, *Wind Effects on Structures*, John Wiley \& Sons, Inc., Third Edition, 1996, 46.

Swarztrauber, Paul and Roland Sweet, (1975), "Efficient fortran subprograms for the solution of elliptic partial differential equations", NCAR Techinical Note, NCAR-TN/IA-109, National Center for Atmospheric Research, Boulder, Colorado, July 1975.